

B-Mesityl Dearomatization

Dearomatizing and Derivatizing a Mesityl Group on Boron by One-Pot Photoisomerization and [4+2] Diels–Alder Addition

Billy Deng, Xiang Wang, and Suning Wang*^[a]

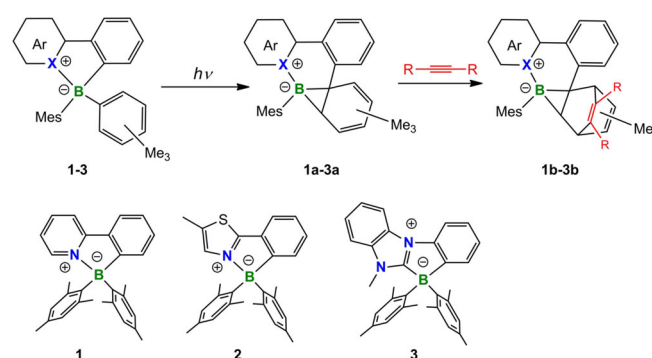
Abstract: Boron compounds having a conjugated chelate backbone (N,C-chelate or C,C-chelate) and two mesityl substituents on boron have been found to undergo a facile one-pot transformation/reaction with dienophiles, which

leads to the dearomatization of one mesityl ring and its [4+2] Diels–Alder addition with the dienophile. Photochemical activation is the key in this transformation of the aryl ring.

Introduction

Arene dearomatization is a powerful approach for generating structurally complex alicyclic building blocks in total synthesis.^[1a] Among the myriad of dearomatization strategies,^[1c,2c] dearomatization by cycloaddition has the advantage of high atom efficiency, and significantly increases the structural complexity in a single step by forming bridged or bicyclic products from simple arenes.^[1] The Diels–Alder (D-A) [4+2] reaction is perhaps the most widely used and versatile mode of cycloaddition in synthetic chemistry.^[2a,b] However, despite its importance, D-A reactions of non-activated monocyclic arenes (e.g., benzene, toluene, mesitylene) continue to pose a synthetic challenge due to their exceptional stability conferred by the aromaticity.^[1b] Typical D-A reactions of non-activated monocyclic arenes require high temperatures/pressures or transition metal catalysts,^[3] or activated dienophiles.^[4] Transition-metal-mediated dearomatization has been extensively explored in recent decades, whereby simple arenes are either η^6 - or η^2 -coordinated to transition metals, enabling their reactivity towards electrophiles in D-A additions under relatively mild conditions.^[3]

Recently, certain boron chelate compounds bearing two aryl substituents on boron have been found to readily undergo quantitative photoisomerization, dearomatizing one aryl group to a cyclodienyl unit that remains η^2 -coordinated to the boron atom. The product could be described as a boratanorcaradiene (BNCD), a 7-borabicyclo[4.1.0]hepta-2,4-diene, or a borirane-fused cyclohexadiene (e.g., **1a–3a** in Scheme 1).^[5] Compared to the chelate starting materials (e.g., **1–3** in Scheme 1), which are thermally stable and chemically inert, the species **1a–3a** are much higher in energy (by ca. 30 kcal mol⁻¹) and their borirane-cyclohexadienyl unit is highly electron-rich and reactive



Scheme 1. Sequential photoisomerization and [4+2] D-A reaction of compounds **1–3**.

towards oxygen.^[5a] We therefore considered the possibility of taking advantage of this photoisomerization to derivatize aryl substituents in molecules such as **1–3**. It was envisaged that this might be achieved by a one-pot process involving initial generation of the BNCD unit by photoisomerization, followed by a [4+2] D-A reaction with an appropriate alkyne or alkene, as illustrated in Scheme 1. To our delight, we found the photochemically generated species **1a–3a** to readily react with electrophilic alkynes/alkenes in a highly stereoselective manner under mild conditions, quantitatively affording the corresponding [4+2] D-A cycloadducts. The unique features of this approach include the absence of transition metal catalysts as well as the mild reaction conditions. The key activation step of this reaction is driven by light, a form of renewable energy. Furthermore, while examples of [4+2] cycloadditions of alkynes^[6] and azides^[7] to boracyclopolyenes have been reported previously, they involve highly reactive boroles. To the best of our knowledge, cycloaddition reactions involving species such as BNCDs have been hitherto unknown.

Herein, we demonstrate a series of stepwise, light-assisted, catalyst-free [4+2] cycloadditions of BNCDs with dienophiles under ambient conditions, affording a series of air-stable, borirane-fused D-A adducts. This new light-driven dearomatization and functionalization of arenes further enriches the metal-free bond-activation chemistry facilitated by boron.^[8]

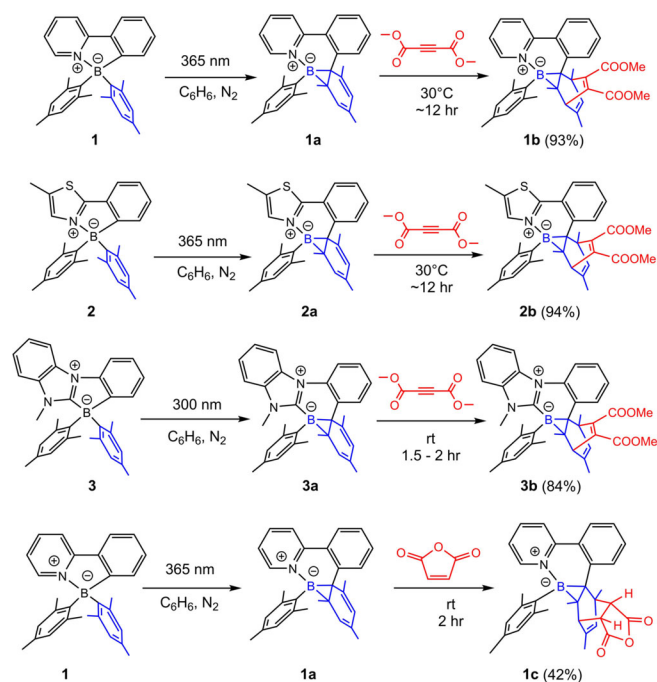
[a] B. Deng, Dr. X. Wang, Prof. Dr. S. Wang
Department of Chemistry, Queen's University
Kingston, Ontario, K7L 3N6 (Canada)
E-mail: sw17@queensu.ca

 Supporting information and the ORCID identification number(s) for the author(s) of this article can be found under:
<https://doi.org/10.1002/chem.201903534>

Results and Discussion

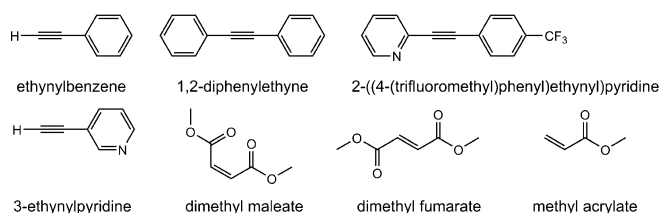
One-pot syntheses of 1b–3b and 1c

Boranes 1–3 were obtained according to previously reported procedures.^[5a–c] They are air-stable and thermally stable. Upon photoirradiation, they can be quantitatively converted to their corresponding dark-coloured isomers. The one-pot procedure used in the present investigation (Scheme 2) involves ini-



Scheme 2. Synthetic routes to compounds 1b–3b and 1c and their isolated yields.

tial photochemical conversion of 1–3 to their respective dark borirane isomers 1a–3a in J-Young NMR tubes, in benzene or toluene, as we have described previously.^[5] This photochemical conversion can be readily tracked by NMR spectroscopy. Upon full conversion to 1a–3a, various dienophiles were examined for their reactivity towards the cyclohexadienyl units therein. Among the alkyne dienophiles we examined, dimethyl acetylenedicarboxylate (DMAD) proved to be the most reactive toward 1a–3a, showing appreciable reactions at ambient temperature, which may be attributed to its relatively high electrophilicity toward the electron-rich dienyl unit. Other alkyne dienophiles, such as those shown in Scheme 3, did not show any



Scheme 3. Dienophiles that failed to react with compounds 1–3.

appreciable reactivity towards 1a–3a at ambient temperature. Because 1a and 2a either undergo rapid thermal reversion to 1 and 2, respectively, or transform to other species at high temperatures,^[5a,b] we restricted the temperature of the reaction with dienophiles to ambient or 30 °C. Compound 3a shows high thermal stability and does not thermally revert back to 3.^[5c] Nonetheless, apart from DMAD, none of the dienophiles in Scheme 3 react with 3, even at elevated temperature (e.g., 100 °C).

The ¹H NMR spectra in Figure 1 demonstrate the quantitative one-pot transformation of 1 into 1b. Irradiating a solution of 1 in benzene (0.04 M) at 365 nm for about 12 h resulted in quantitative conversion into 1a. After the addition of excess DMAD to the solution of 1a and heating the mixture at 30 °C overnight, the D-A product 1b was quantitatively generated. The DMAD starting material (99%, Aldrich) contained unidentified impurities, which could be readily separated from the product by column chromatography on neutral activated alumina. The one-pot conversions of 2 into 2b and of 3 into 3b proceeded in a similar manner (see the Supporting Information), except that for 3 excitation at 300 nm was necessary owing to its considerably blue-shifted absorption bands compared to those of 1 and 2. Interestingly, compared to those with 1a and 2a, the D-A reaction of 3a with DMAD to produce 3b was much faster, reaching completion within a few hours at 30 °C. Considering the strong σ-donating NHC chelate and the high electron density on the borirane ring in 3a, the strong electron-donating substituent on boron accelerates D-A reactions. Compounds 1b–3b proved to be unstable on silica or basic alumina columns, but could be easily purified/isolated on neutral alumina with only a small amount of decomposition. 1b and 2b were obtained as orange crystals, and 3b as light-yellow crystals, from a solvent mixture of hexanes/ethyl acetate. 1b–

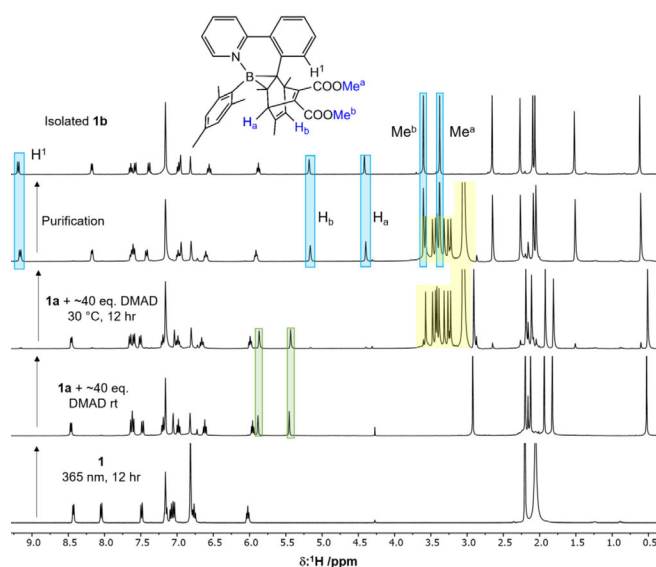


Figure 1. ¹H NMR spectra showing the clean photochemical conversion of 1 into 1a (the green highlighted peaks) and the quantitative formation of 1b (the blue highlighted peaks) after the addition of ca. 40 equiv. of DMAD (the yellow highlighted peak at $\delta = 3.06$ ppm along with associated impurity peaks) to a 0.04 M solution of 1a in C₆D₆.

3b proved to be air-stable and their solutions could be heated at 90 °C overnight under inert conditions without undergoing any changes.

Among the various alkene dienophiles (Scheme 3) that we examined, only maleic anhydride (MA) showed D-A reactivity with the borirane molecule **1a**. The reaction of **1a** with 5 equiv. of MA reached completion in about 20 min at room temperature, quantitatively affording the D-A product **1c**, as shown in Figure 2. **1c** could not be purified by column chro-

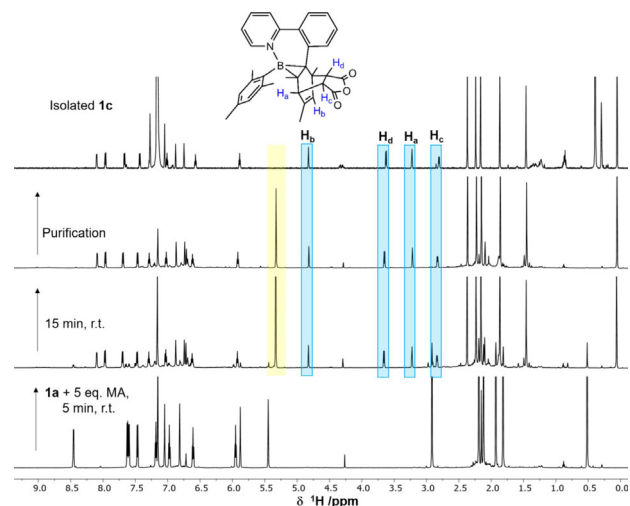


Figure 2. ^1H NMR spectra showing the quantitative formation of **1c** (the blue highlighted peaks) by the reaction of **1a** with 5 equiv. of maleic anhydride (MA, the yellow highlighted peaks, 0.03 M) in C_6D_6 at room temperature.

matography. When the reaction of **1a** with MA was repeated at a 1:1.05 ratio under the same conditions, it reached completion in about 2 h, and without further purification, compound **1c** could be isolated in 42% yield as orange crystals by recrystallization. Compounds **1b–3b** and **1c** were fully characterized by ^1H , ^{13}C , and ^{11}B NMR, HRMS, and single-crystal X-ray diffraction analysis (see the Experimental Section and the Supporting Information for details).

We also examined unsymmetrical molecules,^[9] such as BMe(Ar) chelate compounds, for possible selective aryl activation by the same approach. However, the borirane-cyclohexadienyl units generated from the Ar rings of the unsymmetrical molecules underwent efficient thermal isomerization that effectively competed with the intermolecular D-A additions. We attempted low-temperature photoisomerization of the unsymmetrical boron compounds in order to slow down the undesired thermal isomerization and achieve effective D-A additions. However, only thermal isomerization products were observed, and no [4+2] D-A reactivity was detected for the unsymmetrical boron compounds.

Structures of **1b–3b** and **1c**

Compounds **1b–3b** display distinct ^{11}B NMR peaks at $\delta = -5.7$, -6.3 , and -16.0 ppm, respectively (recorded in C_6D_6), which are downfield-shifted by a few ppm relative to those of **1a**–

3a, as befits saturated borirane structures.^[5,10] Similarly, compound **1c** shows an ^{11}B NMR peak at $\delta = -8.5$ ppm.

The structures of **1b–3b** and **1c** were first determined by comprehensive 2D NMR spectroscopic analysis, which established that the addition of the dienophile to the cyclohexadienyl ring proceeds exclusively from the exposed face of the latter, instead of the cavity between the mesityl and cyclohexadienyl rings, owing to the far lower steric hindrance. The resulting 3-boratricyclo[3.2.2.0^{2,4}]nona-6,8-diene has the *endo* stereogeometry, following the typical [4+2] D-A reaction pathway.^[2] The protons of the Me^d and Me^e groups as well as H_a on the D-A addition unit of **1b** show long-range couplings with one of the methyl groups (Me^f) of the mesityl unit, as shown by the 2D NOESY spectrum in Figure 3. Similar coupling pat-

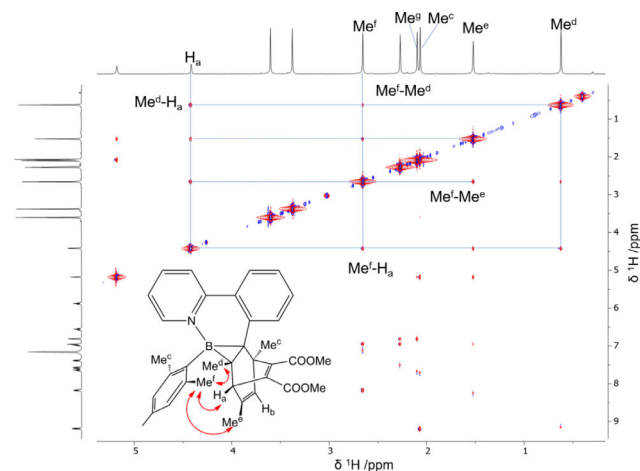


Figure 3. 2D H,H NOESY of **1b** showing the long-range coupling of the protons of Me^f on the mesityl unit with those of the bridged ring (mixing time 0.4 s, recorded in C_6D_6).

terns were also observed in the 2D NOESY spectra of **1c** and **2b** (see the Supporting Information). The signal of *ortho*-H¹ on the phenyl ring of **1b** is unusually downfield shifted, appearing as a doublet at $\delta \approx 9.2$ ppm (Figure 1). The corresponding H¹ protons in compounds **2b** and **3b** show similar chemical shifts (see the Supporting Information). One possible explanation for this is the formation of an H bond between the H¹ atom and one of the carbonyl oxygen atoms. This is indeed confirmed by the crystal structures of **1b–3b**. The borirane species **1a** is known to undergo slow enantiomer interconversion in solution through a 1,3-sigmatropic B–C bond migration, based on the observation of a chemical exchange peak in the NOESY spectrum between the two methyl groups on the sp³ carbon atoms of the borirane unit.^[5a] Interestingly, similar enantiomer interconversion was not observed for **1b**, possibly because of its highly congested nature.

The formation of four new stereogenic centres in **1c** is evident from its ^1H -COSY NMR spectrum (see the Supporting Information). The clean formation of one stereoisomer shown by NMR for **1b–3b** and **1c** also supports the high stereoselectivity of the adduct formation. The absence of a highly deshielded doublet for the *ortho*-H proton on the phenyl ring in **1c** in-

indicates that the carbonyl groups of the anhydride unit are oriented away from the phenyl ring, with exclusive formation of the *endo* adduct.^[11]

The crystal structures of **1b/1c** and **2b/3b** are shown in Figures 4 and 5, respectively. Selected bond lengths and angles are shown in Table 1. The two C=C double bonds in the cycloaddition unit (C4=C5 1.322–1.326 Å, C10=C11 1.341–1.345 Å) of **1b–3b** have typical olefinic bond lengths. The C5=C6 double bond in the cycloaddition unit of **1c** also has a typical C=C bond length of 1.324(3) Å. The crystal structures show that one of the CO₂Me groups (C14 in **1b**, C12 in **2b** and **3b**) is close to the phenyl ring and oriented approximately perpendicular with respect to the C=C bond. Indeed, the carbonyl oxygen atom of this group forms an H bond with an H atom of the phenyl ring (that bound to C17 in **1b** and **2b**, and to C18 in **3b**), as evidenced by the separation distance of 2.18–2.20 Å between the oxygen atom and the H atom. This observation is consistent with the deshielded chemical shift of the H¹ proton of **1b** shown in Figure 1. The crystal structures confirmed the stereogeometry established from the NMR data. The borirane ring remains intact in all four structures. **1b–3b** all have a relatively long B–C bond in the borirane ring (B1–C1 = 1.664(3), 1.695(3), and 1.6976(17) Å for **1b–3b**, respectively). Compared to the previously characterized borirane ring in **3a**, D-A adduct formation increases the B–C_{Ph} bond length in **3b** by about 0.013 Å, which may be ascribed to the increased steric congestion about the B atom. In the adducts **1b–3b**, the bicyclo[2.2.2]octa-2,5-diene unit is approximately perpendicular to

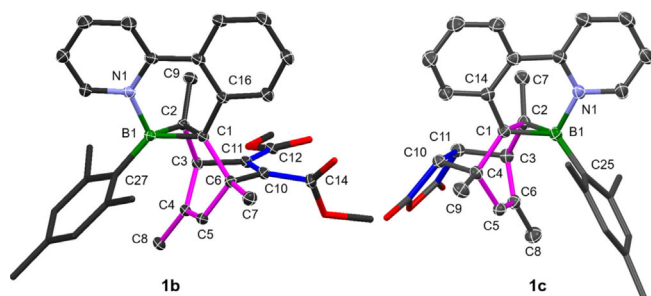


Figure 4. Crystal structures of **1b** and **1c** with a partial labelling scheme and 35% thermal ellipsoids. H atoms are omitted for clarity. The mesityl group and part of the dienophile are shown as sticks.

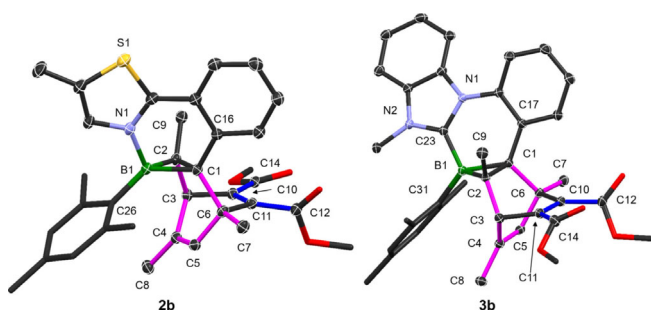


Figure 5. Crystal structures of **2b** and **3b** with a partial labelling scheme and 35% thermal ellipsoids. H atoms are omitted for clarity. The mesityl group and part of the dienophile are shown as sticks.

Table 1. Selected bond lengths (Å) and angles (°) for **1b–3b** and **1c**.

Bond lengths and angles				
1b	B1–C1	1.664(3)	C3–C11	1.521(3)
	B1–C2	1.582(3)	C6–C10	1.550(3)
	B1–N1	1.600(3)	C10–C11	1.341(3)
	B1–C27	1.605(3)	C2–B1–C1	57.09(14)
	C1–C2	1.553(3)	C2–C1–B1	58.80(14)
	C2–C3	1.562(3)	C1–C2–B1	64.11(15)
	C3–C4	1.529(3)	C2–B1–N1	116.28(19)
	C4–C5	1.322(3)	C27–B1–C1	132.04(19)
	C1–C6	1.590(3)	N1–B1–C27	107.77(19)
	C5–C6	1.513(3)	B1–C1–C6	128.09(18)
1c	B1–C1	1.636(3)	C4–C10	1.581(3)
	B1–C2	1.602(3)	C5–C6	1.324(3)
	B1–N1	1.574(3)	C10–C11	1.539(3)
	B1–C25	1.607(3)	C2–B1–C1	57.89(12)
	C1–C2	1.567(3)	C2–C1–B1	59.99(12)
	C1–C4	1.563(3)	C1–C2–B1	62.12(12)
	C2–C3	1.543(3)	N1–B1–C25	109.84(16)
	C2–C7	1.525(3)	N1–B1–C1	112.05(15)
	C3–C11	1.558(3)	C4–C1–B1	120.44(14)
	C3–C6	1.508(3)	C3–C2–B1	124.29(16)
C4–C5	1.518(3)			
2b	B1–C1	1.695(3)	C6–C11	1.546(3)
	B1–C2	1.578(3)	C10–C11	1.341(3)
	B1–C26	1.597(3)	C2–C1–B1	57.99(12)
	B1–N1	1.568(3)	C1–C2–B1	65.57(13)
	C1–C2	1.551(3)	N1–B1–C26	106.93(16)
	C2–C3	1.570(3)	N1–B1–C1	109.31(16)
	C3–C4	1.519(3)	C16–C1–B1	117.63(16)
	C1–C6	1.592(3)	C6–C1–B1	122.80(16)
	C5–C6	1.508(3)	B1–C2–C3	120.33(16)
	C4–C5	1.324(3)		
3b	B1–C1	1.6976(17)	C4–C5	1.3265(18)
	B1–C2	1.5941(17)	C6–C10	1.5517(17)
	B1–C23	1.5969(17)	C10–C11	1.3353(19)
	B1–C31	1.6092(18)	C10–C11	1.3353(19)
	C1–C2	1.5316(16)	C2–B1–C1	55.35(7)
	C1–C6	1.5813(16)	C2–C1–B1	58.89(7)
	C2–C3	1.5705(17)	C1–C2–B1	65.76(8)
	C3–C4	1.5268(17)	C2–B1–C23	121.35(10)
	C4–C5	1.3265(18)	C2–B1–C31	124.08(10)
	C5–C6	1.5138(17)	C3–C2–B1	119.53(10)
C3–C11	1.5195(17)	C23–B1–C31	108.33(10)	
C6–C10	1.5517(17)			

the borirane ring. The cyclohexene bridge (pink) (e.g., in **1b**, C3–C4–C5–C6) is bent away from the bridgehead (C3–C11–C10–C6 in **1b**) towards the mesityl unit.

The structure of **1c** (Figure 4) shows that the maleic anhydride unit in the adduct is indeed oriented away from the phenyl ring without any intramolecular H-bond interactions. This preferred orientation is likely dictated by the need to minimize steric interactions between the phenyl ring and the anhydride unit.

Absorption spectra of **1b–3b** and **1c**

The absorption spectra of **1b–3b** and **1c**, along with those of **1a–3a**, are shown in Figure 6. For **1b**, **1c**, and **2b**, the first

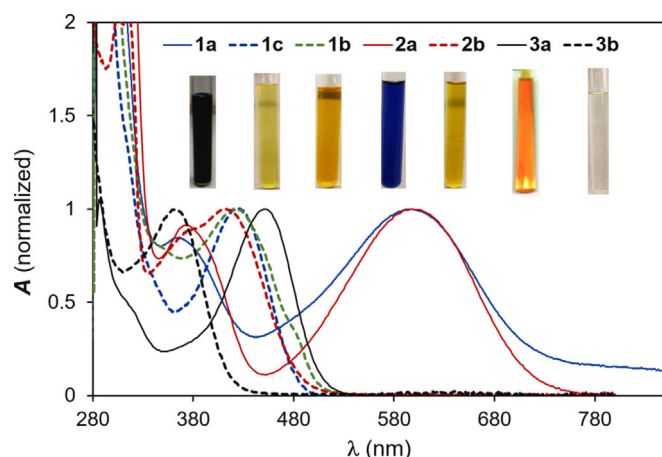


Figure 6. Absorption spectra of **1a–3a**, **1b–3b**, and **1c** recorded in benzene (normalized with respect to the first low-energy band). Inset: photographs showing the solution colours of these compounds in benzene.

low-energy absorption band appears at $\lambda_{\max} \approx 420$ nm, which is responsible for the yellow-orange colour of these three compounds. In contrast, the first low-energy absorption band of **3b** is hypsochromically shifted by about 60 nm relative to those of **1b** and **2b**, making it pale-yellow. Compared to the cyclohexadienyl borirane parent molecules **1a**, **2a**, and **3a**, which are much more intensely coloured, with the first absorption band appearing at around 600 nm for **1a** and **2a** and at 454 nm for **3a**, the first absorption bands of the D-A borirane species **1b–3b** and **1c** are sharply hypsochromically shifted. This difference is caused by the unsaturated dienyl unit directly attached to the borirane ring in **1a–3a**, which significantly contributes to the HOMO level, along with the borirane ring, raising the HOMO energy level such that these compounds display reactivity toward oxygen.^[5] In **1b–3b/1c**, D-A addition converts the unsaturated sp^2 carbon atoms attached to the borirane ring into sp^3 carbon atoms, which presumably greatly reduces the contribution of the D-A unit to the HOMO level and the electron density on the borirane unit, leading to a stabilized HOMO and an increased HOMO–LUMO gap. To further understand the electronic properties of **1b–3b/1c**, TD-DFT computational studies were performed at the B3LYP/6–311G(d) level of theory.^[12] HOMO–LUMO diagrams for **1b–3b/1c** are shown in Figure 7.

Consistent with their absorption spectra, the calculated HOMO–LUMO gaps of **1b** and **1c** are significantly larger (3.47 eV and 3.43 eV, respectively) than that of their precursor **1a** (2.32 eV).^[5a] TD-DFT data indicate that the vertical excitation to the S_1 state for **1b** and **1c** is dominated by the HOMO to LUMO transition with an energy of around 2.85 eV, approximately 0.90 eV higher than that of **1a**. Similar trends are also found for **2b** vs **2a** and **3a** vs **3b** (see the Supporting Information). As shown in Figure 7, the LUMO levels for **1b–3b** and **1c** are mainly localized on their chelate backbones. Unlike in **1a–3a**, in which the HOMO is dominated by the borirane and the cyclohexadienyl ring,^[5a] the key contributions to the HOMOs of **1b** and **1c** stem from the mesityl ring and the C=C bonds in the D-A adduct, which are clearly responsible for the widening

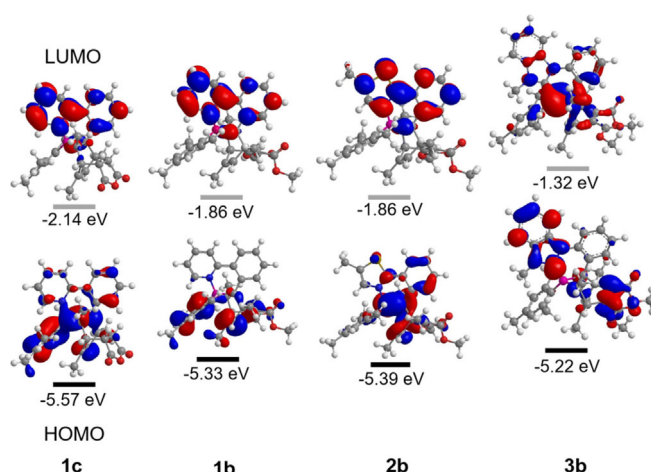


Figure 7. HOMOs and LUMOs of **1c** and **1b–3b** with an iso-contour of 0.03 for all surfaces.

of their HOMO–LUMO gaps. For **2b** and **3b**, although there are significant contributions from the borirane ring to the HOMO, the contributions from the D-A adduct unit to the HOMO are very small, leading to a widening of their HOMO–LUMO gaps relative to those of **2a** and **3a**. In contrast to the instability of **1a–3a** toward oxygen, the relatively deeper HOMOs of **1b–3b** and **1c** (stabilized by ca. 1 eV) make these compounds stable to air. Furthermore, unlike their precursors **1a–3a**, which are either thermally or photochemically active, compounds **1b–3b** and **1c** do not show any thermal or photoreactivities upon heating to 100 °C or irradiation at around λ_{\max} of their first low-energy absorption band.

Conclusions

Photochemical transformation of an aromatic mesityl group on boron has been established as an effective method for activating it toward facile Diels–Alder addition reactions with dienophiles in a one-pot manner. This type of photo-initiated aryl activation has been found to be a general reactivity for BMe_2 units with different diaryl chelate backbones. The clean photochemical conversion of the BMe_2 chelate compounds into the corresponding cyclohexadienyl-fused boriranes is the key step in this type of aryl activation.

Experimental Section

General

Unless stated otherwise, all reactions were carried out under an inert atmosphere of dry nitrogen in sealed J-Young NMR tubes (conventional DURAN® glass). Starting reagents were purchased from chemical suppliers and used without further purification. Deuterated benzene (C_6D_6) was purchased from Cambridge Isotope Laboratories and purged with dry nitrogen and stored over molecular sieves prior to use. NMR spectra were recorded at 298 K using the following spectrometers: Bruker Avance 400, Neo 500, Avance 600, or Neo 700. Abbreviations: s=singlet, d=doublet, dd=doublet of doublets, t=triplet, td=triplet of doublets, m=

multiplet, High-resolution mass spectra were recorded on a Thermo Fisher Scientific MALDI LTQ Orbitrap XL mass spectrometer. Exact masses were calculated based on the predominant combination of natural isotopes. Photoisomerization reactions of all compounds were performed in sealed J-Young NMR tubes using a Rayonet photochemical reactor at 298 K. UV/Vis spectra were recorded on a Varian Cary 50 spectrophotometer.

Synthesis and characterization

Synthesis of 1b: Compound **1** was synthesized according to a previous literature procedure.^[5a] **1** (15 mg, 37 μ mol) was dissolved in C₆D₆ (0.90 mL, *c* = 0.04 M) and irradiated at ambient temperature with UV lamps at 365 nm for 8 h to fully convert colourless **1** into dark-blue **1a**, as monitored by ¹H NMR spectrometry. DMAD (0.1 mL, 0.82 mmol) was then added in a single portion to the solution of **1a**. After heating overnight in an oil bath at 30 °C, the solution turned yellow and NMR spectra indicated nearly quantitative formation of **1b**. The clear yellow solution containing the product was concentrated in vacuo and purified by column chromatography on neutral alumina eluting with hexanes/ethyl acetate (9:1), affording a yellow-orange residue. Crystals of **1b** were grown by slow evaporation of the volatiles from a concentrated solution in hexanes/ethyl acetate (5:1) and subsequently washed with hexanes to afford the pure product (19 mg, 93%). ¹H NMR (400 MHz, C₆D₆): δ = 9.19 (d, *J* = 8.3 Hz, 1H; *o*-Cbz-H), 8.18 (dd, *J* = 6.5, 1.7 Hz, 1H; *o*-Py-H), 7.64 (t, *J* = 7.5 Hz, 1H; *m*-3-Cbz-H), 7.58 (d, *J* = 8.2 Hz, 1H; *m*-5-Cbz-H), 7.39 (d, *J* = 8.5 Hz, 1H; *m*-5-Py-H), 6.99 (t, *J* = 7.6 Hz, 1H; *p*-Cbz-H, overlapped with Mes-H), 6.95 (s, 1H; Mes-H, overlapped with *p*-Cbz-H), 6.82 (s, 1H; Mes-H), 6.56 (td, *J* = 8.3 Hz, 1.6 Hz, 1H; *p*-Py-H), 5.88 (t, *J* = 6.8 Hz, 1H; *m*-3-Py-H), 5.18 (s, 1H; cyclohexene-sp²-C-H), 4.42 (d, ⁴*J* = 2.0 Hz, 1H; cyclohexene-sp³-C-H), 3.60 (s, 3H; -OCH₃), 3.38 (s, 3H; -OCH₃), 2.66 (s, 3H; *o*-Mes-2-CH₃), 2.27 (s, 3H; *p*-Mes-CH₃), 2.10 (s, 3H; *o*-Mes-6-CH₃), 2.07 (s, 3H; cyclohexene-CH₃), 1.52 (d, ⁴*J* = 1.06 Hz, 3H; allylic CH₃), 0.62 ppm (s, 3H; BCC-CH₃); ¹³C NMR (126 MHz, C₆D₆): δ = 169.49, 165.57, 160.24, 151.70, 148.61, 147.82, 147.61, 145.80, 145.64, 141.40, 140.24, 137.12, 136.20, 134.33, 131.61, 130.39, 127.98, 127.88, 127.69, 127.49, 126.28, 125.78, 122.94, 120.95, 119.93, 54.80, 52.52, 51.47, 51.04, 29.88, 23.68, 23.16, 20.92, 20.56, 20.05, 16.58 ppm; ¹¹B NMR (128 MHz, C₆D₆): δ = -5.77 ppm; HREI-MS: calcd for C₃₅H₃₆BNO₄ [M]⁺: 545.2737; found: 545.2738.

Synthesis of 2b: Compound **2** was synthesized according to a previous literature report.^[5b] **2** (22 mg, 51 μ mol) was dissolved in C₆D₆ (2 mL, *c* = 0.025 M) and irradiated with UV light at 365 nm for 7 days to fully convert it into **2a**. DMAD (0.1 mL, 0.82 mmol) was then added in a single portion to the solution of **2a**. After heating overnight in an oil bath at 30 °C, the clear yellow solution containing the product was concentrated in vacuo and purified by column chromatography on neutral alumina eluting with hexanes/ethyl acetate (9:1), affording a yellow residue of **2b**. Crystals of **2b** were grown by slow evaporation of the volatiles from a concentrated solution in hexanes/ethyl acetate (5:1) and washed with hexanes to afford the pure compound (28 mg, 94%). ¹H NMR (700 MHz, C₆D₆): δ = 9.23 (d, *J* = 8.5 Hz, 1H; *o*-Cbz-H), 7.56 (td, *J* = 7.8, 7.2, 1.3 Hz, 1H; *m*-3-Cbz-H), 7.49 (dd, *J* = 7.8, 1.1 Hz, 1H; *m*-5-Cbz-H), 6.95 (s, 1H; Mes-H), 6.86 (t, *J* = 7.5 Hz, 1H; *p*-Cbz-H), 6.84 (s, 1H; Mes-H), 6.75 (d, *J* = 1.4 Hz, 1H; thiazole-H), 5.28 (t, *J* = 2.0 Hz, 1H; cyclohexene-sp²-C-H), 4.45 (d, *J* = 2.2 Hz, 1H; cyclohexene-sp³-C-H), 3.62 (s, 3H; -OCH₃), 3.38 (s, 3H; -OCH₃), 2.66 (s, 3H; *o*-Mes-2-), 2.27 (s, 3H; *p*-Mes-CH₃), 2.16 (s, 3H; *o*-Mes-6-CH₃), 2.08 (s, 3H; cyclohexene-CH₃), 1.42 (d, ⁴*J* = 1.7 Hz, 3H; allylic CH₃), 1.16 (d, ⁴*J* = 1.2 Hz, 3H; thiazole-CH₃), 0.59 ppm (s, 3H; BCC-CH₃); ¹³C NMR (176 MHz, C₆D₆): δ = 169.90, 165.83, 162.79, 159.64, 148.53, 147.59,

141.03, 140.90, 137.40, 136.92, 134.74, 134.31, 132.22, 131.16, 129.04, 128.20, 128.06, 127.92, 127.10, 123.90, 123.17, 54.65, 52.50, 51.87, 51.44, 23.90, 23.89, 21.30, 20.32, 20.27, 16.33, 11.15 ppm; ¹¹B NMR (128 MHz, C₆D₆): δ = -6.32 ppm; HREI-MS: calcd for C₃₄H₃₆BNO₄ [M]⁺: 565.2458; found: 565.2473.

Synthesis of 3b: Compound **3** was synthesized according to a previous literature procedure.^[5c] Compound **3** (4.0 mg, 9 μ mol) was solubilized in C₆D₆ (0.51 mL, *c* = 0.017 M) and irradiated with UV light at 300 nm for 3 h to fully convert it into **3a**. DMAD (0.1 mL, 0.82 mmol) was then added to the reaction mixture in a single portion. After heating in an oil bath at 30 °C for 2 h, the clear light-yellow solution containing the product was concentrated in vacuo and purified by column chromatography on neutral alumina eluting with hexanes/ethyl acetate (9:1), affording a light-yellow residue of **3b**. Crystals of **3b** were grown by slow evaporation of the volatiles from a concentrated solution in hexanes/dichloromethane (9:1) and washed with hexanes to afford the pure compound (4.4 mg, 84%). ¹H NMR (700 MHz, C₆D₆): δ = 9.39 (d, *J* = 8.0 Hz, 1H; *o*-Cbz-H), 7.68 (d, *J* = 8.0 Hz, 1H), 7.65–7.61 (m, 1H; Cbz-*N*-(Ph)C=C-H), 7.61 (t, *J* = 8.0 Hz, 1H; *m*-3-Cbz-H), 7.05 (t, *J* = 8.5 Hz, 1H; *p*-Cbz-H, overlapped with a C₆D₆ satellite peak), 6.85 (s, 1H; Mes-H), 6.84–6.80 (m, 2H; BzIm-H), 6.73 (s, 1H; Mes-H), 6.44–6.40 (m, 1H; CH₃-N-(Ph)C=C-H), 5.27 (t, *J* = 2.0 Hz, 1H; cyclohexene-sp²-C-H), 4.43 (d, *J* = 2.2 Hz, 1H; cyclohexene-sp³-C-H), 3.60 (s, 3H; -OCH₃), 3.41 (s, 3H; -OCH₃), 2.75 (s, 3H; *o*-Mes-CH₃), 2.49 (s, 3H; *N*-CH₃), 2.29 (s, 3H; *p*-Mes-CH₃), 2.00 (s, 3H; cyclohexene-CH₃), 1.86 (s, 3H; *o*-Mes-6-CH₃), 1.49 (d, ⁴*J* = 1.59, 3H; allylic CH₃), 0.88 ppm (s, 3H; BCC-CH₃); ¹³C NMR (176 MHz, C₆D₆): δ = 170.01, 165.91, 162.37, 150.67, 145.78, 142.71, 141.30, 137.18, 136.60, 136.60, 135.58, 133.70, 132.71, 132.37, 130.18, 128.45, 128.20, 128.06, 127.92, 126.13, 124.14, 123.74, 123.09, 118.67, 114.45, 110.28, 56.46, 53.63, 51.87, 51.44, 31.50, 30.23, 24.86, 23.75, 21.91, 21.31, 20.70, 19.76 ppm; ¹¹B NMR (225 MHz, C₆D₆): δ = -15.96 ppm; HREI-MS: calcd for C₃₈H₃₉BNO₄ [M]⁺: 598.3003; found: 598.3001.

Synthesis of 1c: Compound **1a** (8.8 mg, 21.8 μ mol, 30 mM, 0.5 mL of C₆D₆) was generated in the same manner as described for the synthesis of **1b**. Maleic anhydride (2.20 mg, 22 μ mol) was added to the reaction mixture in a single portion. After 24 h at room temperature, the clear yellow solution was concentrated in vacuo and then extracted with hexanes to afford a yellow residue of **1c**. Crystals of **1c** were grown by slow evaporation of the solvent from a concentrated solution in hexanes and washed with cold hexanes to afford the pure compound (42%). ¹H NMR (700 MHz, C₆D₆): δ = 8.10 (d, *J* = 6.4 Hz, 1H; *o*-Py-H), 7.96 (d, *J* = 8.4 Hz, 1H; *o*-Cbz-H), 7.67 (d, *J* = 8.2 Hz, 1H; *m*-5-Cbz-H), 7.43 (d, *J* = 8.6 Hz, 1H; *m*-5-Py-H), 7.29–7.26 (m, 1H; *m*-2-Cbz-H), 7.01 (t, *J* = 7.6 Hz, 1H; *p*-Cbz-H), 6.88 (s, 1H; Mes-H), 6.75 (s, 1H; Mes-H), 6.57 (t, *J* = 7.8 Hz, 1H; *p*-Py-H), 5.89 (t, *J* = 6.8 Hz, 1H; *m*-2-Py-H), 4.82 (t, *J* = 1.9 Hz, 1H; cyclohexene-sp²-C-H), 3.63 (d, *J* = 8.1 Hz, 1H; *exo*-H), 3.23 (t, *J* = 2.6 Hz, 1H; cyclohexene-sp³-C-H), 2.81 (dd, *J* = 8.1, 3.2 Hz, 1H; *exo*-H), 2.37 (s, 3H; *o*-Mes-CH₃), 2.24 (s, 3H; *p*-Mes-CH₃), 2.16 (s, 3H; cyclohexene-CH₃), 1.87 (s, 3H; *o*-Mes-CH₃), 1.46 (d, *J* = 1.6 Hz, 3H; allylic CH₃), 0.05 ppm (s, 3H; BCC-CH₃); ¹³C NMR (176 MHz, C₆D₆): δ = 173.95, 173.09, 146.02, 145.51, 141.75, 140.21, 139.54, 136.07, 136.01, 135.14, 130.17, 129.96, 128.59, 128.20, 128.06, 127.92, 127.41, 122.62, 121.16, 120.45, 49.92, 49.09, 44.32, 43.36, 23.64, 23.56, 23.30, 21.83, 21.23, 13.97 ppm; ¹¹B NMR (225 MHz, C₆D₆): δ = -8.70 ppm; HRESI-MS: calcd for C₃₃H₃₂BNO₃ [M+1]: 502.2548; found: 502.2536.

X-ray crystallographic analysis

Crystal data for **1b–3b** and **1c** were collected on a Bruker D8 Venture diffractometer with an Mo target ($\lambda = 0.71073 \text{ \AA}$) at 180 K. Data were processed on a PC with the aid of the Bruker SHELXTL software package^[13] and corrected for absorption effects. The crystals of **1b**, **1c**, and **2b** belong to the triclinic space group $P\bar{1}$, whereas that of **3b** belongs to the monoclinic space group $P2_1/n$. All non-hydrogen atoms were refined anisotropically. The positions of hydrogen atoms were calculated and their contributions were included in the structural factors. Full details of the crystal data, collection parameters, and results of analyses are provided in the Supporting Information. Crystal data for **1b–3b** and **1c** have been deposited with the Cambridge Crystallographic Data Centre. CCDC 1943914 (**1b**), 1943915 (**2b**), 1943916 (**3b**), and 1943917 (**1c**) contain the supplementary crystallographic data for this paper. These data can be obtained free of charge from the Cambridge Crystallographic Data Centre.

Computational study

DFT and TD-DFT calculations were performed using the Gaussian 09 suite of programs^[12] and computational facilities provided by Compute Canada. Geometry optimizations and vertical excitations of all compounds were obtained at the B3LYP/6-31g(d) level of theory, using crystal structural data as the initial geometrical parameters.

Acknowledgements

We thank the Natural Sciences and Engineering Research Council of Canada for financial support.

Conflict of interest

The authors declare no conflict of interest.

Keywords: arene ligands · boriranes · dearomatization · Diels–Alder addition · photoisomerization · synthetic methods

- [1] a) S. P. Roche, J. A. Porco, *Angew. Chem. Int. Ed.* **2011**, *50*, 4068–4093; *Angew. Chem.* **2011**, *123*, 4154–4179; b) W. C. Wertjes, E. H. Southgate, D. Sarlah, *Chem. Soc. Rev.* **2018**, *47*, 7996–8017; c) F. C. Pigge, in *Arene Chemistry* (Ed.: J. Mortier), Wiley, Hoboken, **2015**, pp. 399–423.
- [2] a) F. Fringuelli, A. Taticchi, *The Diels–Alder Reaction: Selected Practical Methods*, Wiley, Chichester, **2002**; b) K. C. Nicolaou, S. A. Snyder, T. Montagnon, G. Vassilikogiannakis, *Angew. Chem. Int. Ed.* **2002**, *41*, 1668–1698; *Angew. Chem.* **2002**, *114*, 1742–1773; c) C. X. Zhuo, W. Zhang, S. L. You, *Angew. Chem. Int. Ed.* **2012**, *51*, 12662–12686; *Angew. Chem.* **2012**, *124*, 12834–12858.
- [3] a) M. F. Semmelhack, A. Chlenov, *Transition Metal Arene π -Complexes in Organic Synthesis and Catalysis*, Springer, Heidelberg, **2004**; b) A. R. Pape, K. P. Kaliappan, E. P. Kündig, *Chem. Rev.* **2000**, *100*, 2917–2940; c) B. K. Liebov, W. D. Harman, *Chem. Rev.* **2017**, *117*, 13721–13755; d) M. S. Bailey, B. J. Brisdon, D. W. Brown, K. M. Stark, *Tetrahedron Lett.* **1983**, *24*, 3037–3040; e) M. D. Chordia, P. L. Smith, S. H. Meiere, M. Sabat, W. D. Harman, *J. Am. Chem. Soc.* **2001**, *123*, 10756–10757; f) W. D. Harman, *Chem. Rev.* **1997**, *97*, 1953–1978.
- [4] a) Y. Inagaki, M. Nakamoto, A. Sekiguchi, *Nat. Commun.* **2014**, *5*, 3018; b) X. Li, S. J. Danishefsky, *J. Am. Chem. Soc.* **2010**, *132*, 11004–11005; c) F. Fringuelli, O. Piermatti, F. Pizzo, L. Vaccaro, *Eur. J. Org. Chem.* **2001**, 439–455.
- [5] a) Y. L. Rao, H. Amarne, S. Bin Zhao, T. M. McCormick, S. Martić, Y. Sun, R. Y. Wang, S. Wang, *J. Am. Chem. Soc.* **2008**, *130*, 12898–12900; b) Y. L. Rao, H. Amarne, L. D. Chen, M. L. Brown, N. J. Mosey, S. Wang, *J. Am. Chem. Soc.* **2013**, *135*, 3407–3410; c) Y. L. Rao, L. D. Chen, N. J. Mosey, S. Wang, *J. Am. Chem. Soc.* **2012**, *134*, 11026–11034; d) K. Nagura, S. Saito, R. Fröhlich, F. Glorius, S. Yamaguchi, *Angew. Chem. Int. Ed.* **2012**, *51*, 7762–7766; *Angew. Chem.* **2012**, *124*, 7882–7886; e) Y.-L. Rao, C. Hörl, H. Braunschweig, S. Wang, *Angew. Chem. Int. Ed.* **2014**, *53*, 9095–9096; *Angew. Chem.* **2014**, *126*, 9243–9243.
- [6] a) C. Fan, W. E. Piers, M. Parvez, R. McDonald, *Organometallics* **2010**, *29*, 5132–5139; b) J. J. Eisch, J. E. Galle, *J. Am. Chem. Soc.* **1975**, *97*, 4436–4437; c) J. J. Eisch, J. E. Galle, B. Shafii, A. L. Rhelngold, *Organometallics* **1990**, *9*, 2342–2349; d) H. Kelch, S. Kachel, J. Wahler, M. A. Celik, A. Stoy, I. Krummenacher, T. Kramer, K. Radacki, H. Braunschweig, *Chem. Eur. J.* **2018**, *24*, 15387–15391; e) J. J. Baker, K. H. M. Al Furajji, O. T. Liyanage, D. J. D. Wilson, J. L. Dutton, C. D. Martin, *Chem. Eur. J.* **2019**, *25*, 1581–1587.
- [7] a) H. Braunschweig, C. Hörl, L. Mailänder, K. Radacki, J. Wahler, *Chem. Eur. J.* **2014**, *20*, 9858–9861; b) S. A. Couchman, T. K. Thompson, D. J. D. Wilson, J. L. Dutton, C. D. Martin, *Chem. Commun.* **2014**, *50*, 11724–11726.
- [8] a) A. R. Jupp, D. W. Stephan, *Trends Chemistry* **2019**, *1*, 35–48; b) M. A. Légaré, G. Bélanger-Chabot, R. D. Dewhurst, E. Welz, I. Krummenacher, B. Engels, H. Braunschweig, *Science* **2018**, *359*, 896–900; c) M.-A. Légaré, M.-A. Courtemanche, E. Rochette, F. G. Fontaine, *Science* **2015**, *349*, 513–516; d) D. W. Stephan, G. Erker, *Angew. Chem. Int. Ed.* **2015**, *54*, 6400–6441; *Angew. Chem.* **2015**, *127*, 6498–6541; e) A. J. Warner, A. Churn, J. S. McGough, M. J. Ingleson, *Angew. Chem. Int. Ed.* **2017**, *56*, 354–358; *Angew. Chem.* **2017**, *129*, 360–364; f) K. Yuan, S. Wang, *Org. Lett.* **2017**, *19*, 1462–1465; g) S. Kirschner, S.-S. Bao, M. K. Fengel, M. Bolte, H.-W. Lerner, M. Wagner, *Org. Biomol. Chem.* **2019**, *17*, 5060–5065; h) E. C. Neeve, S. J. Geier, I. A. I. Mkhaliid, S. A. Westcott, T. B. Marder, *Chem. Rev.* **2016**, *116*, 9091–9161.
- [9] S. K. Mellerup, C. Li, T. Peng, S. Wang, *Angew. Chem. Int. Ed.* **2017**, *56*, 6093–6097; *Angew. Chem.* **2017**, *129*, 6189–6193.
- [10] a) H. Braunschweig, C. Claes, A. Damme, A. Deißberger, R. D. Dewhurst, C. Hörl, T. Kramer, *Chem. Commun.* **2015**, *51*, 1627–1630; b) P. Bis-singer, H. Braunschweig, K. Kraft, T. Kupfer, *Angew. Chem. Int. Ed.* **2011**, *50*, 4704–4707; *Angew. Chem.* **2011**, *123*, 4801–4804; c) C. Balzereit, C. Kybart, H. J. Winkler, W. Massa, A. Berndt, *Angew. Chem. Int. Ed. Engl.* **1994**, *33*, 1487–1489; *Angew. Chem.* **1994**, *106*, 1579–1581; d) S. W. Denmark, K. Nishide, A. M. Faucher, *J. Am. Chem. Soc.* **1991**, *113*, 6675–6676; e) T. R. McFadden, C. Fang, S. J. Geib, E. Merling, P. Liu, D. P. Curran, *J. Am. Chem. Soc.* **2017**, *139*, 1726–1729.
- [11] a) Z. Goldschmidt, S. Antebi, H. E. Gottlieb, D. Cohen, U. Shmueli, Z. Stein, *J. Organomet. Chem.* **1985**, *282*, 369–381; b) F. K. Brown, K. N. Houk, D. J. Burnell, Z. Valenta, *J. Org. Chem.* **1987**, *52*, 3050–3059; c) E. Vogel, H. Günther, *Angew. Chem. Int. Ed. Engl.* **1967**, *6*, 385–401; *Angew. Chem.* **1967**, *79*, 429–446.
- [12] Gaussian 09, Revision A.02, M. J. Frisch, G. W. Trucks, H. B. Schlegel, G. E. Scuseria, M. A. Robb, J. R. Cheeseman, G. Scalmani, V. Barone, G. A. Petersson, H. Nakatsuji, X. Li, M. Caricato, A. Marenich, J. Bloino, B. G. Janesko, R. Gomperts, B. Mennucci, H. P. Hratchian, J. V. Ortiz, A. F. Izmaylov, J. L. Sonnenberg, D. Williams-Young, F. Ding, F. Lipparini, F. Egidi, J. Goings, B. Peng, A. Petrone, T. Henderson, D. Ranasinghe, V. G. Zakrzewski, J. Gao, N. Rega, G. Zheng, W. Liang, M. Hada, M. Ehara, K. Toyota, R. Fukuda, J. Hasegawa, M. Ishida, T. Nakajima, Y. Honda, O. Kitao, H. Nakai, T. Vreven, K. Throssell, J. A. Montgomery, Jr., J. E. Peralta, F. Ogliaro, M. Bearpark, J. J. Heyd, E. Brothers, K. N. Kudin, V. N. Staroverov, T. Keith, R. Kobayashi, J. Normand, K. Raghavachari, A. Rendell, J. C. Burant, S. S. Iyengar, J. Tomasi, M. Cossi, J. M. Millam, M. Klene, C. Adamo, R. Cammi, J. W. Ochterski, R. L. Martin, K. Morokuma, O. Farkas, J. B. Foresman, D. J. Fox, Gaussian, Inc., Wallingford CT, **2016**.
- [13] SHELXTL, version 6.14; Bruker AXS, Madison, WI, **2000–2003**.

Manuscript received: August 2, 2019

Accepted manuscript online: September 5, 2019

Version of record online: ■■■■■ 0000

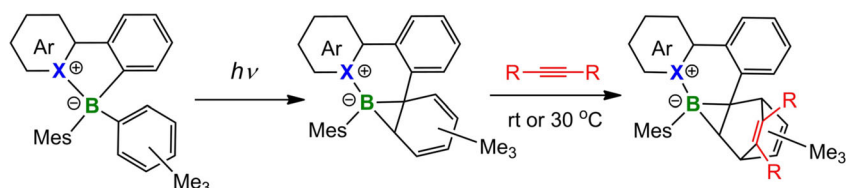
FULL PAPER

B-Mesityl Dearomatization

B. Deng, X. Wang, S. Wang*



Dearomatizing and Derivatizing a Mesityl Group on Boron by One-Pot Photoisomerization and [4+2] Diels–Alder Addition



Dearomatization of boron-bound arenes: One-pot photochemical activation of an aryl ring on boron and subsequent [4+2] Diels–Alder addition with

dienophiles leads to clean conversion of the aryl ring to a 3-boratricyclo[3.2.2.0^{2,4}]nona-6,8-diene (see graphic).